Available online at www.eccomasproceedia.org
Eccomas Proceedia UNCECOMP (2017) 690-705

ECCOMAS
Proceedia

UNCECOMP 2017
2nd ECCOMAS Thematic Conference on
Uncertainty Quantification in Computational Sciences and Engineering
M. Papadrakakis, V. Papadopoulos, G. Stefanou (eds.)
Rhodes Island, Greece, 15–17 June 2017

STOCHASTIC MULTI-OBJECTIVE OPTIMISATION OF COMPOSITES MANUFACTURING PROCESS

K. I. Tifkitsis[1], **A. A. Skordos**[1]

[1] School of Aerospace, Transport and Manufacturing, Cranfield University
Bedford, MK430AL, UK
e-mail: {k.tifkitsis, a.a.skordos}@cranfield.ac.uk

Keywords: composite materials, uncertainty quantification, stochastic simulation, surrogate model, stochastic multi-objective optimisation

Abstract. *This paper addresses the development of a stochastic multi-objective optimisation methodology and its implementation in the manufacturing of thick composite parts. Boundary conditions variability was quantified conducting a series of experiments and stochastic objects have been developed representing these uncertainties. The stochastic optimisation scheme takes into account the uncertainty of process parameters and boundary conditions and identifies optimal solutions that minimise process outcomes such as process duration and extent of defect formation and their uncertainty. The Kriging method was implemented to construct a computationally efficient surrogate model of manufacturing based on sample points selected by the Latin Hypercube Sampling (LHS) method and generated by a Finite Element (FE) model of the process. Response surfaces were constructed to test the accuracy of the surrogate model against the FE solution. A Genetic Algorithm (GA) was utilised to solve the multi-objective optimisation problem. The surrogate model was coupled with Monte Carlo (MC) and integrated into the stochastic multi-objective optimisation framework. The results show that a significant reduction in process duration and process induced defects variability in comparison with conventional processing conditions of up to 80% and 40% respectively can be achieved by the optimisation.*

Peer-review under responsibility of the organizing committee of UNCECOMP 2017.
doi: 10.7712/120217.5404.16763

1 INTRODUCTION

Thermosetting matrix fibrous composites have been widely utilised in a variety of applications in industry due to their excellent mechanical properties combined with low weight. The cure process, which is the last stage of thermosetting composite fabrication, is a non-linear heat transfer phenomenon, during which the exothermic reaction transforms the matrix from an oligomeric liquid to a glassy solid. This spontaneous cross linking reaction results in the generation of a significant amount of heat which, in addition to the low thermal conductivity of the material in the through thickness direction, can lead to significant thermal gradients. Temperature overshoots can result in material degradation and excessive thermal stresses which can be critical in the case of high temperature operation [1]. Also, thermal gradients through the thickness lead to non-uniformity of degree of cure.

Conventional manufacturing processes reduce the probability of significant exothermic phenomena by using conservative thermal profiles. These usually involve long dwell at relatively lower temperatures, which naturally result in long process durations and high manufacturing costs. In this context, multi-objective optimisation of composites manufacturing offers an opportunity for the minimisation of potential cure process-induced defects and cost. The selection of optimal cure profiles in order to minimise cure time and cure process-induced defects has been investigated as a single-objective optimisation problem [2-4] whilst the multi-objective problem has been addressed recently [3] showing a trade-off behaviour with an L shape Pareto front formed by process designs that minimise temperature overshoot and process duration. A number of these solutions represent considerable improvements in both process time and temperature overshoot.

The manufacture of composite materials involves many parameters presenting considerable variability [4]. This variability induces uncertainty into the manufacturing process and affects its outcome. These uncertainties can also initiate process defects resulting in significantly amount of rejected parts associated with considerable cost. Stochastic simulation methodologies have recently started to be developed in order to address the uncertainties in composites manufacture and to investigate their influence in process outcomes such as cure time, geometrical distortion and temperature overshoot. The cure process includes different sources of variability in process parameters (cure kinetics) and boundary conditions (heat transfer coefficient, tool temperature). Cure kinetics parameters variability has been quantified experimentally using Differential Scanning Calorimetry (DSC) [5]. The initial degree of cure, activation energy and reaction order present significant variability introducing a coefficient of variation of approximately 30% in temperature overshoot and resulting in potential defects into the cured part. In terms of boundary conditions, experiments and stochastic models have shown carried out for the quantification of boundary conditions variability in an infusion process [6]. Stochastic models developed representing this variability integrated with an existing model of cure kinetics uncertainty to examine variability impact in the process outcomes. The surface heat transfer and tool temperature variability cause significant variability in cure time reaching a coefficient of variation of approximately 20% [6]. Tool temperature variability has the greatest influence on process outcome [7] whilst, higher levels of uncertainty increase the optimal cure time [8].

A stochastic multi-objective optimisation framework has been developed in the present study integrating a stochastic simulation method (Monte Carlo scheme) and a Genetic Algorithm (GA) in order to minimise the cure process time and temperature overshoot as well as their uncertainty. The manufacturing process boundary conditions (convection heat transfer coefficient, surface temperature) variability has been quantified experimentally. Stochastic objects representing the boundary conditions variability have been developed and incorporated into the stochastic simulation scheme. A surrogate model was developed using the Kriging method

replacing the FE model and reducing significantly the computational effort. The methodology is applied to the case of a thick flat carbon fibre-epoxy laminate.

2 METHODOLOGY

2.1 Cure Simulation

A thermal cure simulation model was developed in the finite element solver MSC.Marc to simulate the curing stage of an infusion process in an oven. Figure 1 depicts a schematic representation of the model geometry and boundary conditions. The model represents a flat composite panel and comprises 26 3D iso-parametric eight-node composite brick elements of type 175 in MSC.Marc for thermal analysis [9]. Each element comprises two plies of Hexcel G1157 pseudo unidirectional carbon fibre reinforcement with 0.3 mm nominal thickness. Consequently, the overall thickness of the flat laminate is 15.6 mm. The matrix is Hexcel RTM6 epoxy resin. The boundary conditions illustrated in Figure 1 are implemented using user subroutines FORCDT and UFILM for time dependent prescribed temperature and forced air convection respectively [10]. A two dwell cure profile as shown in Figure 2 is applied on the lower surface of the composite part by selecting the following parameters; 1st dwell temperature T_1, 2nd dwell temperature T_2, 1st and 2nd dwell time dt_1 and dt_2 respectively, and ramp rate r. Due to the symmetry across the width of the part, the heat transfer model was solved as a transient 1D heat transfer problem. The initial condition was considered to be 2% degree of cure and uniform temperature after the end of filling. User subroutines UCURE, USPCHT, and ANKOND were utilised for the integration of material sub-models, cure reaction kinetics, specific heat capacity and thermal conductivity respectively [10].

The cure kinetics model is a combination of an nth order model an autocatalytic model [11]. The cure reaction rate in is calculated as follows:

$$\frac{da}{dt} = k_1(1-a)^{n_1} + k_2(1-a)^{n_2}a^m \quad (1)$$

where a is the current degree of cure, m, n_1, n_2 the reaction orders, k_1 and k_2 the reaction rate constants following an Arrhenius law:

$$k_1 = A_1 e^{(-E_1/RT)} \quad (2)$$

$$k_2 = A_2 e^{(-E_2/RT)} \quad (3)$$

where A_1, A_2 denote pre-exponential factors, E the activation energy and R the universal gas constant. Model constants values are reported in [12].

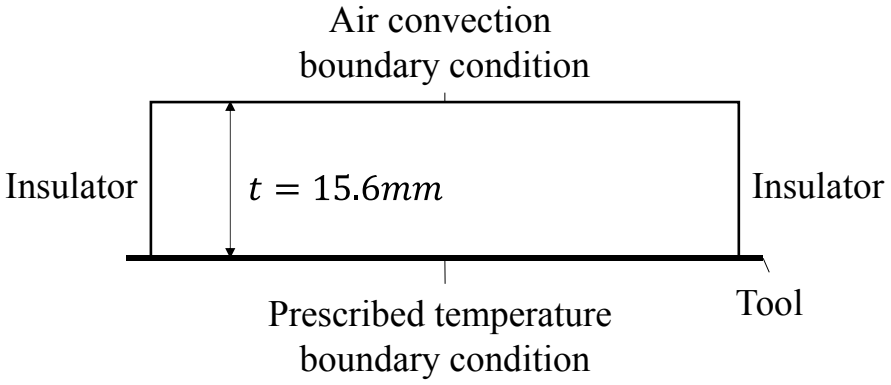

Figure 1 Model schematic representation.

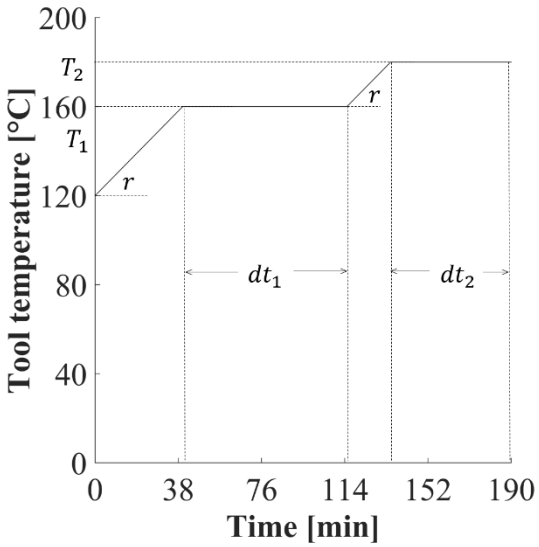

Figure 2 Two-dwell cure profile.

The specific heat capacity of the resin and the fibre is calculated using experimental data obtained by modulated differential scanning calorimetry [2]. The specific heat capacity of the composite is computed making use of the rule of mixtures as follows:

$$c_p = w_f c_{pf} + \left(1 - w_f\right) c_{pr} \tag{4}$$

where w_f is the fibre weight fraction, c_{pf} the fibre specific heat capacity and c_{pr} the specific heat capacity of the resin. The thermal conductivity of the anisotropic composite material in the longitudinal direction is computed using an appropriate geometry-based model [13] and can be expressed as follows:

$$K_{11} = v_f K_{lf} + (1 - v_f) K_r \tag{5}$$

where v_f is the fibre volume fraction, K_{lf} and K_r are the thermal conductivity of the fibre in the longitudinal direction and of the resin, respectively. In the transverse direction the thermal conductivity is calculated as follows:

$$K_{22} = K_{33} = v_f K_r \left(\frac{K_{tf}}{K_r} - 1\right) + K_r \left(\frac{1}{2} - \frac{K_{tf}}{2K_r}\right) + K_r \left(\frac{K_{tf}}{K_r} 1\right) \sqrt{{v_f}^2 - v_f + \frac{\left(\frac{K_{tf}}{K_r} + 1\right)^2}{\left(\frac{2K_{tf}}{K_r} - 2\right)^2}} \tag{6}$$

where K_{tf} is the thermal conductivity of the fibre in the transverse direction.

2.2 Surrogate model

The utilisation of FE analysis for the simulation of cure requires high computational time. In terms of stochastic simulation and multi-objective optimisation problems, the use of FE model becomes computationally highly demanding. A surrogate model was constructed using the Kriging method to address this high computational effort replacing the FE-model. Figure 3 shows the procedure of surrogate model development. The Kriging method requires a set of input points and their responses generated using FE analysis. Latin Hypercube Sampling (LHS) [14], a random sample generation method, was chosen for generating a sample of 15000 input values and their responses. In this study, the 1st and 2nd dwell temperature, 1st dwell time, heat

transfer coefficient, reaction order and activation energy have been considered as input parameters. Table 1 presents the input ranges of the initial design space. The outputs of the surrogate model are the cure time and temperature overshoot. Cure time is considered as the time at which the minimum degree of cure of the part is greater than 0.88, which is the degree of cure at which the epoxy resin (RTM6) reaches during an isothermal cure at 180°C, whilst temperature overshoot is the maximum difference between tool temperature and local temperature of the laminate during curing.

Kriging allows the estimation of untried parameters values to be made without bias and with minimum variance and more accurately in comparison with low order polynomial regression models [15].

Given a set of m design sites

$$S = [s_1\ s_2 \cdots s_m]^{\mathrm{T}} \text{ with } s_i \in \mathbb{R}^n \tag{7}$$

and responses

$$Y = [y_1\ y_2 \cdots y_m]^{\mathrm{T}} \text{ with } y_i \in \mathbb{R}^q \tag{8}$$

The data is assumed to satisfy the normalisation conditions

$$\mu\left[S_{:,j}\right] = 0, \qquad V\left[S_{:,j}, S_{:,j}\right] = 1, j = 1, \ldots, n \tag{9}$$

$$\mu\left[Y_{:,j}\right] = 0, \qquad V\left[Y_{:,j}, Y_{:,j}\right] = 1, j = 1, \ldots, q \tag{10}$$

where $\mu[\cdot]$ and $V[\cdot,\cdot]$ denote the mean and the covariance respectively.

The Kriging model treats the deterministic response vector $y(x) \in \mathbb{R}^q$, for a n dimensional input $x \in \mathcal{D} \subseteq \mathbb{R}^n$ as a realisation of a regression model $\mathcal{F}$ and a random field,

$$\hat{y}_l(x) = \mathcal{F}\left(\beta_{:,l}, x\right) + z_l(x), l = 1, \ldots, q \tag{11}$$

The regression model $\mathcal{F}$ is a linear combination of p chosen functions $f_j(x)$: $\mathbb{R}^n \longmapsto \mathbb{R}$,

$$\begin{aligned} \mathcal{F}\left(\beta_{:,l}, x\right) &= \beta_{1,l} f_1(x) + \cdots \beta_{p,l} f_p(x) \\ &= \left[f_1(x) \cdots f_p(x)\right]\beta_{:,l} \\ &\equiv f(x)^{\mathrm{T}} \beta_{:,l} \end{aligned} \tag{12}$$

where the coefficients $\{\beta_{p,l}\}$ are regression parameters.

The random field z is assumed to have mean zero and covariance

$$E[z_l(w) z_l(x)] = \sigma_l^2 R(\theta, w, x), \qquad l = 1, \ldots, q \tag{13}$$

where σ_l^2 is the field variance for the l^{th} component of the response and $R(\theta, w, x)$ is the correlation surface with parameter vector θ.

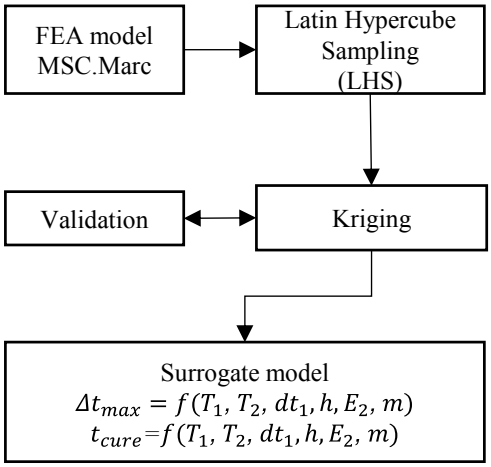

Figure 3 Surrogate model construction methodology.

Table 1 Range of surrogate model input parameters.

Parameters	Range
T_1[°C]	135-175
T_2[°C]	175-215
$dt_1[min]$	42-300
$h[W/m^2/°C]$	13.8-21.8
$E_2[J/mol]$	56020-59620
m	1.008-1.572

For the set S of design sites, an $m \times p$ design matrix F can be constructed with $F_{ij} = f_j(s_i)$,

$$F = [f(s_1) \cdots f(s_m)]^{\mathrm{T}} \tag{14}$$

The $m \times p$ correlation matrix R can be constructed as

$$R_{ij} = \mathcal{R}(\theta, s_i, s_j), \qquad i,j = 1,\ldots,m \tag{15}$$

The fitted regression parameter β^*, a $p \times q$ matrix, can be calculated considering matrices F and R, using least squares as follows:

$$\beta^* = (F^{\mathrm{T}} R^{-1} F)^{-1} F^{\mathrm{T}} R^{-1} Y \tag{16}$$

For any untried design point x, the vector $r(x)$ of correlations between different z at design sites and x, can be defined as

$$r(x) = [\,\mathcal{R}(\theta, s_1, x) \cdots \mathcal{R}(\theta, s_m, x)]^{\mathrm{T}} \tag{17}$$

Therefore, the Kriging predictor is

$$\hat{y}(x) = f(x)^{\mathrm{T}} \beta^* + r(x)^{\mathrm{T}} \gamma^* \tag{18}$$

where the $m \times q$ matrix γ^*can be calculated through the residuals,

$$R\gamma^* = Y - F\beta^* \tag{19}$$

Matrices β^* and $\gamma^*$are fixed for a fixed set of design data. Only vectors $f(x) \in \mathbb{R}^p$ and $r(x) \in \mathbb{R}^m$ have to be computed for every new x.

Correlation models can be divided into two groups, those containing functions that have a parabolic behaviour near the origin (Gaussian, Cubic and Spline), and those including functions with a linear behaviour near the origin (exponential, linear and spherical). The curing stage is a continuously differentiable phenomenon resulting in a parabolic behaviour of correlation function close to origin. Therefore, a Gaussian function and a 2nd order polynomial were selected for the correlation and the regression model respectively. Coefficients β^* and $\gamma^*$of Eq. (19), the 2nd order regression and the Gaussian correlation function respectively, were calculated using the Matlab toolbox for Kriging modelling [16]. The surrogate model was implemented in C++.

2.3 Experimental set-up for the quantification of boundary conditions uncertainty

The uncertainty of boundary conditions was investigated by carrying out a series of experiments using an infusion set-up placed inside in an oven. These experiments aim to quantify the variability of the air temperature in the oven and of the surface heat transfer coefficient between the vacuum bag and the air.

Ten experiments were conducted, utilising the set-up depicted in Figures 4 and 5. It comprises a CALTHERM E9321V2 oven with an EUROTHERM 2408P4 PID controller, a 10 mm aluminium plate, a nylon N64PS-x VAC INNOVATION peel ply fabric, a nylon xR1.2 VAC INNOVATION vacuum bag, two K-type thermocouples and two RdF micro-foil heat flux sensors [17].

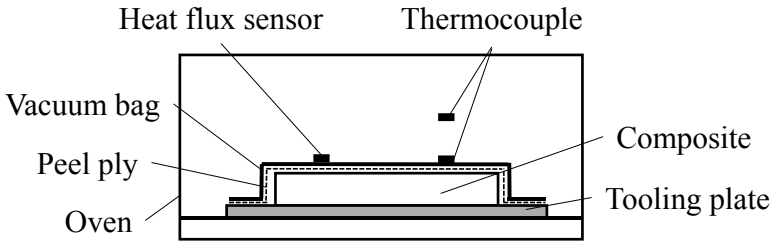

Figure 4 Schematic representation of experimental set-up.

A carbon fibre-epoxy flat panel fabricated by infusion process was utilised to produce thermal conditions similar to those during the cure of a part. The resin system of the panel was Hexcel RTM6, whilst the preform was Hexcel AS7 6k carbon fibre [18] with an areal density of 280 g/m^2. The composite part was placed on the tooling plate, covered with the peel ply and the vacuum bag and sealed before experimental runs.

The flux sensors were placed on the vacuum bag to measure the forced convection variability as well as its spatial dependence. A K-type thermocouple was mounted on the bag to measure the surface temperature, whilst a second sensor was placed close to surface but outside the thermal boundary layer to monitor air temperature. The temperature was set-up at 160 °C in all tests. A National Instruments LabVIEW in house code was utilised for data acquisition and the data were acquired with a frequency of 0.8 Hz.

The micro-foil flux sensor consists of a thin layer, and is a differential thermocouple sensor using T-type thermocouples [17]. The sensor measures the temperature on both sides of the thin layer, which are used to calculate the heat gain or loss through the thin layer. The same heat flux should flow through the sensor and the surface where the sensor is placed. The sensor output is a voltage signal which is proportional to heat flux. Specifically, the heat flux $\dot{Q}$ is calculated by the following relation:

$$\dot{Q} = (H/(C\,TF) \tag{20}$$

where H is the sensor output, whilst C and TF are a calibration multiplier and a temperature multiplication factor respectively, and are provided by the manufacturer. The sensors used in these experiments have a calibration multiplier of 0.15 μV/W/m^2. The temperature multiplication factor is a function of temperature and can be found in [17]. The heat transfer coefficient h was calculated using the temperatures of the surface T_s and air in the oven T_{air} as follows:

$$h = \frac{\dot{Q}}{T_s - T_{air}} \tag{21}$$

a) b)

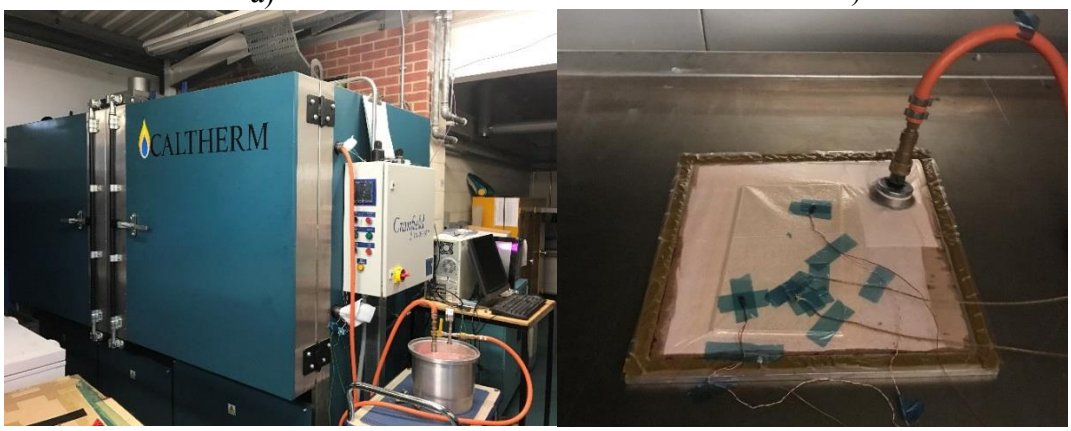

Figure 5 a) CALTHERM E9321V2 oven with a EUROTHERM 2408P4 PID controller and data acquisition system b) infusion set up with the sensors.

2.4 Stochastic simulation

The stochastic simulation was carried out using a Monte Carlo (MC) scheme. This method involves generation of random input stochastic variables using a random number generator. The deterministic model is executed a number of times for each set of inputs and the process outcomes are analysed in term of their probability distributions. The simulation requires a certain number of iterations to ensure the convergence in mean and standard deviation.

2.5 Stochastic multi-objective optimisation

The aim of stochastic optimisation is to minimise cure time and temperature overshoot and their variability by optimising the cure profile parameters. An interface has been developed incorporating MC simulation into a Genetic algorithm (GA) for multi-objective optimisation. A two dwell cure profile depicted in Figure 2 has been considered and parametrised using three parameters; temperature of first and second dwell and the duration of the first dwell. The ranges of potential values for each parameter used in optimisation are summarised in Table 2. It should be noted that the ramp rate r and second dwell time dt_2 are not considered as design parameters in order to reduce the dimensionality of the problem and are equal to 2 °C/min and dt_1 respectively. The minimisation objectives of the optimisation are the mean values and standard deviations of t_{cure} and ΔT_{max}. Figure 6 summarises the steps the stochastic optimisation methodology. The GA begins by generating the first population of individuals. A Monte Carlo simulation is carried out using the surrogate model for each individual calculating the mean value and the standard deviation of cure time and maximum temperature overshoot. A new population is generated by a number of operations (crossover, mutation) based on the previous population individuals. The GA finishes when a convergence criterion is satisfied and the output is a matrix of the optimal points called Pareto front.

Table 2 Design parameters ranges

Parameters	Range
T_1[°C]	135-175
T_2[°C]	175-215
$dt_1[min]$	42-300

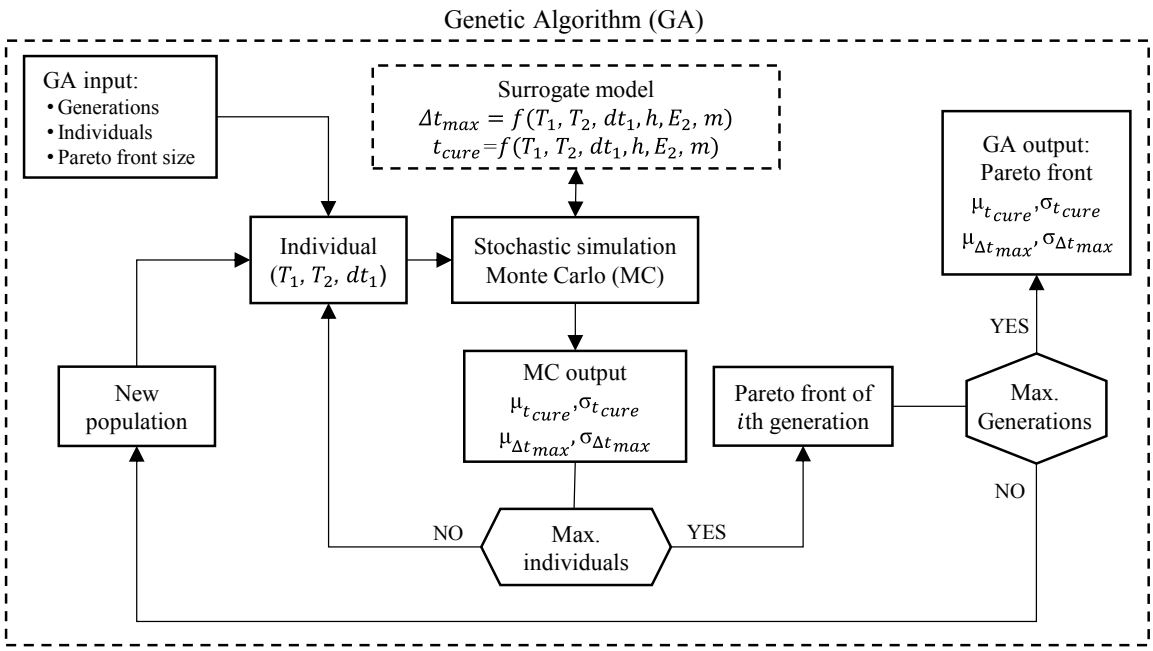

Figure 6 Stochastic multi-objective optimisation framework.

3 RESULTS

3.1 Validation of surrogate model

Figure 7a shows the dependence of t_{cure} on T_1 and dt_1, for constant T_2, h, m and E_2 equal to 195 °C, 17.82 W/m^2/°C, 1.29 and 57820 J/mol respectively. The response of the surrogate model is in good agreement with the response of the FE model, with an average absolute difference of 0.56 min. The response surface shows a trade-off between dt_1 and t_{cure} especially in the region of low T_1. Figure 7b illustrates the response surface of temperature overshoot as a function of the first and second dwell temperature using the surrogate and FE model. In this case the dwell time is equal to 83 min and the remaining input parameters h, m and E_2 as reported in the previous case. The average absolute difference is 0.69 °C, showing the high accuracy of the surrogate model. The overshoot increases as a function of T_1. A global minimum of temperature overshoot is reached for a T_1 in the 140-145 °C range. In this case the first dwell advances the chemical reaction as much as possible in order to minimise temperature overshoots in the second dwell. The overshoot increases slightly for first dwell temperatures below 140 °C as the temperature is too low to advance the resin reaction during the first dwell sufficiently to supress generation of higher exothermic effects during the second dwell.

The use of the surrogate model addresses problems related to computational time, specifically in the case of stochastic simulations where a large number of iterations is required. A typical two-dwell cure profile was utilised as input for Monte Carlo where the number of model runs was equal to 1000. Figures 8a and 8b show the cumulative density functions (CDFs) of cure time and temperature overshoot respectively, calculated both by the FE and surrogate models. It can be observed that the two CDFs are in a good agreement.

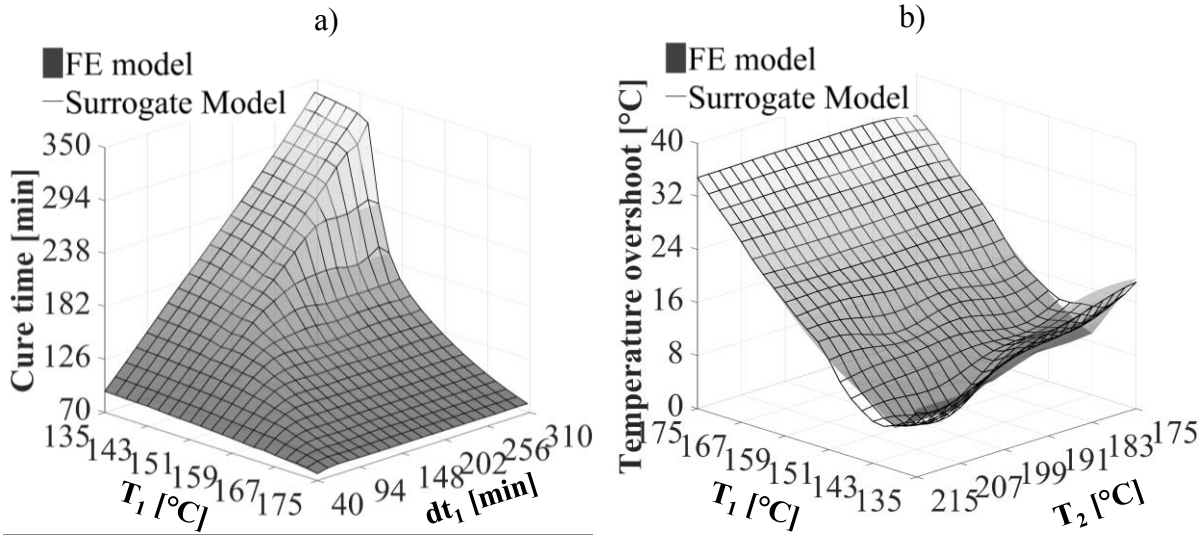

Figure 7 Response surfaces a) cure time as a function of 1st dwell temperature and 1st dwell time b) temperature overshoot as a function of 1st and 2nd dwell temperature.

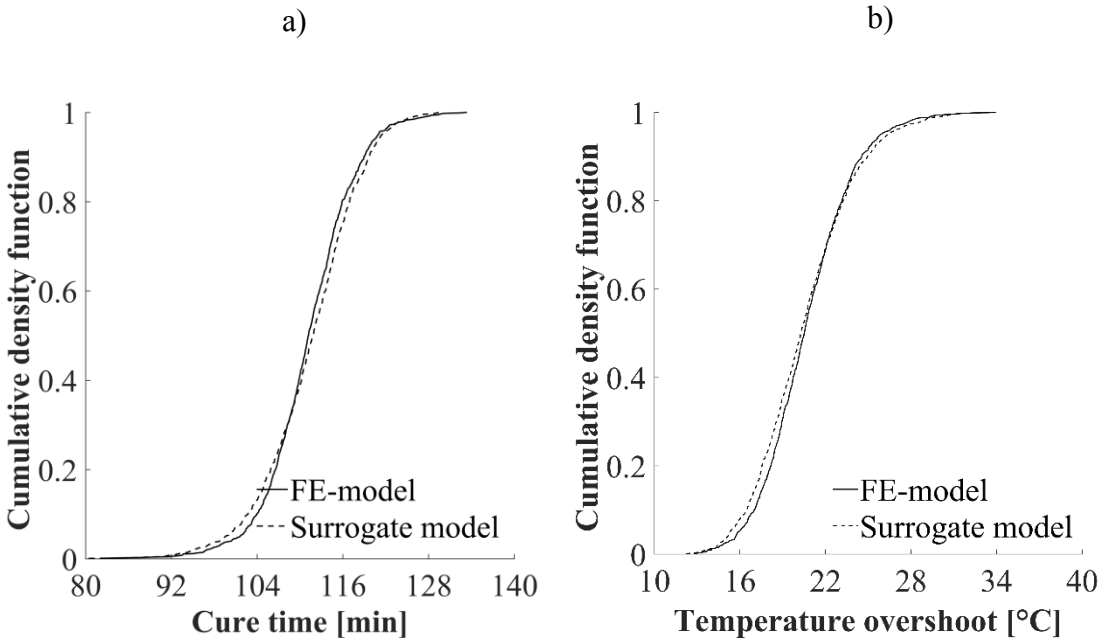

Figure 8 Cumulative density functions (CDFs) of a standard two dwell cure profile; a) CDF of cure time b) CDF of temperature overshoot.

3.2 Experimental results

Figures 9a and 9b summarise the experimental data of heat transfer coefficient and surface temperature evolution over time respectively for ten different runs. Both T_s and h present significant variability across different runs. The short term variability can be attributed to the motion of the air streams inside the oven due to the fan rather than to signal noise effects. The surface temperature presents a periodic term over time caused by the temperature controller of the oven and short term variability due to random variations. The results of surface heat transfer coefficient show only short term variability and a variable level across the runs. These variations can be attributed to the fact that the air movement is forced by the fan in the oven.

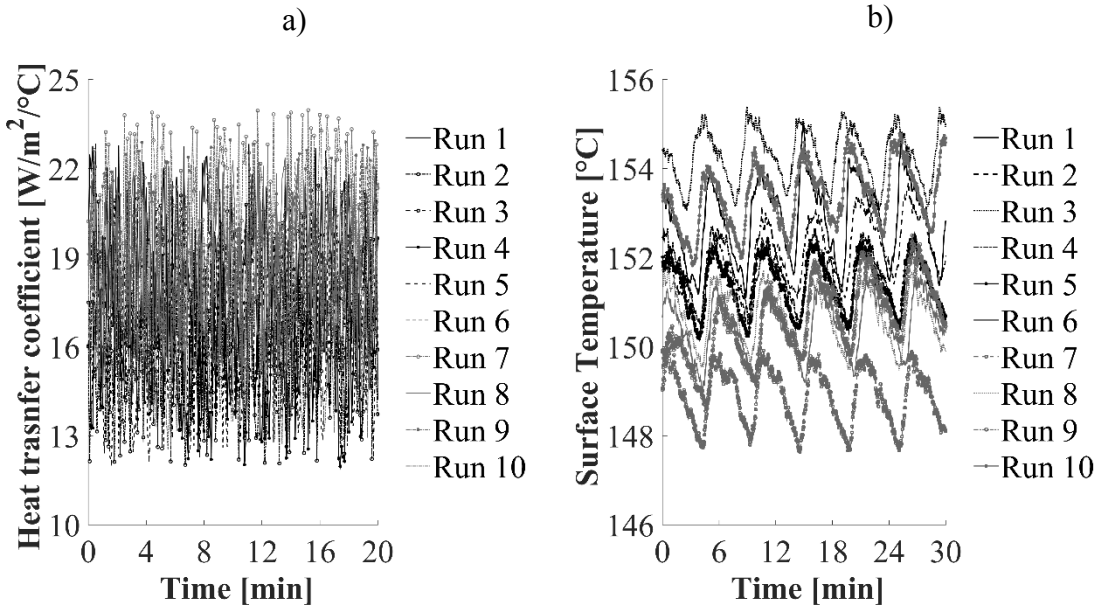

Figure 9 Experimental results of a) heat transfer coefficient b) surface temperature.

3.3 Stochastic objects development

Fast Fourier Transformation (FFT) implemented in MATLAB was utilised to calculate the frequency of T_s. Then, a cosinusoidal fit as shown in Figure 10 was performed making use of generalised reduced gradient non-linear optimisation method implemented in MS Excel [19] calculating the amplitude of the periodic trend. Consequently, detrending was applied in order to generate a stationary process of surface temperature. The Ornstein-Uhlenbeck process (OU), which is a mean reverting second order stationary Gaussian process, was utilised to represent the surface temperature after detrending. The stochastic differential equation of OU process can be written as follows [20]:

$$dS = \lambda(\mu - S)dt + \sigma dW_t \tag{22}$$

where S is the OU process, W_t a Brownian motion following a normal distribution with mean 0 and standard deviation 1 so that $W_t \sim N(0,1)$, whilst dW_t follows a normal distribution with average 0 and standard deviation $\sqrt{dt}$ so that $W_t \sim N(0, \sqrt{dt})$, λ controls the speed of reversion to the long term average of the process, σ is the process volatility and μ is the long term mean of the stochastic process. The analytical solution of Eq. (22) has been used in this study to develop the stochastic object of surface temperature and can be written as follows [20]:

$$S_t = e^{-\lambda \Delta t} S_{t-1} + \left(1 - e^{-\lambda \Delta t}\right)\mu + \sigma \sqrt{\frac{(1 - e^{-2\lambda \Delta t})}{2\lambda}} W_t \tag{23}$$

where Δt is the time increment.

This procedure was repeated for each experimental run. The stochastic process of surface temperature can be expressed as follows:

$$T_s = A_s + B_s cos\, \omega_s t + S_s \tag{24}$$

where A_s is the level of each experimental curve, B_s and ω_s the amplitude and frequency of the cosinusoidal fit respectively, and S_s the mean reverting stationary stochastic process (OU) calculated by Eq. (23). The surface heat transfer coefficient does not involve a periodic trend and can be modelled as realisation of a random scalar variable as follows:

$$h = A_h + B_h y \tag{25}$$

where A_h is the level, B_h the volatility of the process for each run, and y is a standard normal variable. The statistical properties as calculated from the different experimental run are presented in Table 3.

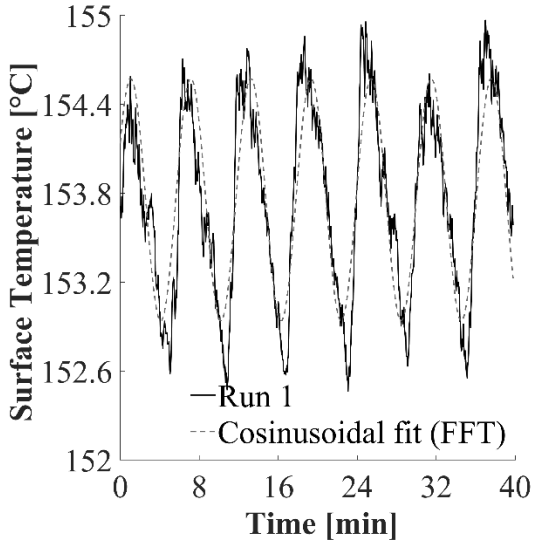

Figure 10 Cosinusoidal fit of surface temperature

Table 3 Statistical properties of boundary conditions.

Boundary conditions	Stochastic model parameter	Mean	Standard deviation
$h\ [(W/m^2)/°C]$	A_h	17.82	1.33
	B_h	2.1	0.1
T_s[°C]	A_s	152	1.64
	B_s	0.82	0.086
	ω_s	0.02	0.0003
	λ_s	0.97	0.4
	σ_s	0.4	0.052
	μ_s	0.007	0.022

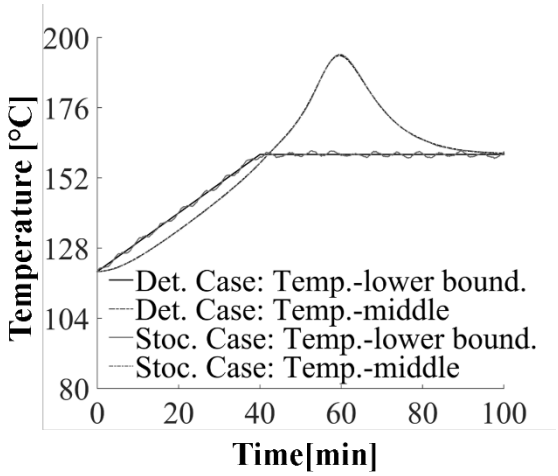

Figure 11 Surface temperature variability over time.

The FE model, described in section 2.1 was used with a time increment of 3 sec to represent short term phenomena. The stochastic simulation was compared with the deterministic model to evaluate the significance of short term variability. Figure 11 shows the temperature evolution with time at the bottom and the middle of the composite part for both stochastic and deterministic model. The temperature at the bottom of the part presents a short term variability with negligible influence of variability.

A number of stochastic simulation iterations have been carried out to calculate the average and standard deviation of cure time and temperature overshoot over time. It was found that the mean value of cure time and temperature overshoot are 94.9 min and 34.6 °C with standard deviations 0.07 min and 0.3 °C respectively. The cure time and temperature overshoot of the deterministic model were 95 min and 34 °C, indicating the negligible influence of short term variability of surface temperature. Similarly, heat transfer coefficient short term variability does not affect the cure time and the temperature overshoot.

According to these results, the stochastic simulation can be carried out considering the variability of the level of surface temperature and surface heat transfer coefficient. Therefore Eq. (24) and (25) can be expressed as follows:

$$T_s = A_s \tag{26}$$

$$h = A_h \tag{27}$$

Furthermore, the variability of cure kinetics is controlled by the reaction order m, and activation energy E_2 (Eqs. (1),(3)) [12]. Tables 4 and 5 summarise the statistical properties and the correlation matrix of m and E_2 respectively.

Table 4 Statistical properties of stochastic cure kinetics parameters.

Parameters	Mean	Standard deviation
m	1.29	0.094
E_2 $[J/mol]$	57820	600

Table 5 Correlation matrix.

Parameters	m	E_2 $[J/mol]$
m	1	0.55
E_2 $[J/mol]$	-0.84	1

3.4 Stochastic simulation

A Monte Carlo simulation has been carried out for the standard two dwell cure profile [21] in order to investigate the variability of cure time and temperature overshoot. The nominal two dwell cure profile comprises one dwell temperature at 160 °C with duration 75 min and a second dwell temperature at 180 °C for 75 min, whilst the ramp rate is equal to 1 °C/min. The surface temperature T_1 and T_2, surface heat transfer coefficient h, activation energy E_2 and reaction order m have been considered as stochastic objects. Figure 12a illustrates the results of Monte Carlo for cure time. The mean time converges after 100 iterations and is 111 min, considerably faster than standard deviation which converges after about 500 iterations and is equal to 7.5 min. The results of temperature overshoot are illustrated in Figure 12b. The mean value converges after 100 iterations to 20.5 °C, whilst the standard deviation converges after 400 runs to 3.4 °C. Cure time and temperature overshoot of the standard cure profile present coefficients of variation of 6% and 16.5% respectively, necessitating a thorough investigation of a solution not only with the minimum value but with minimum uncertainty.

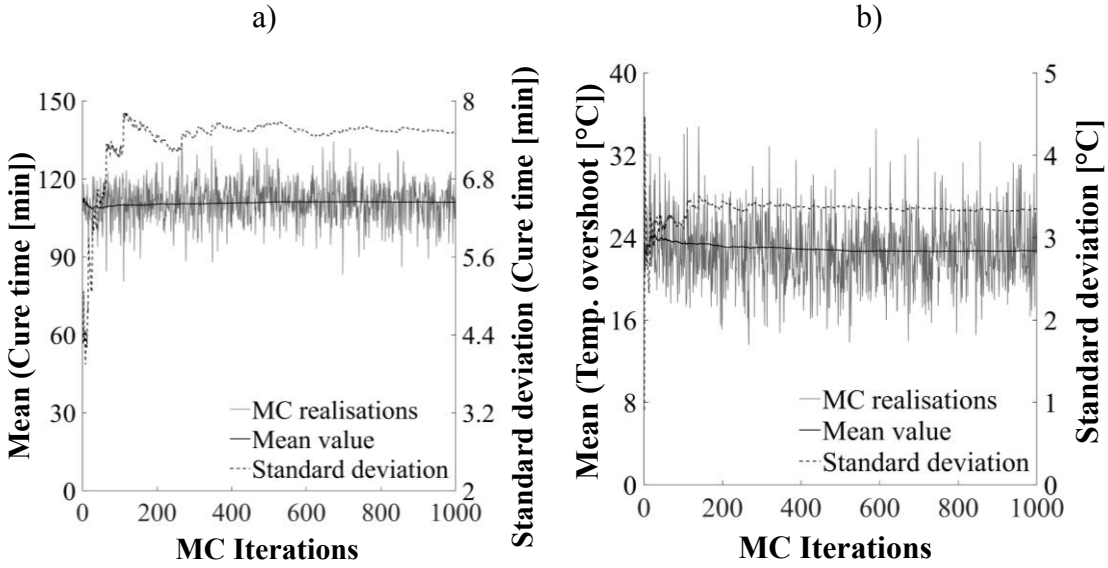

Figure 12 Monte Carlo simulation results a) Cure time [min] b) Temperature overshoot [°C].

3.5 Stochastic multi-objective optimisation

A deterministic two-objective optimisation was carried out using the nominal values of input parameters. Figures 13a and 13b illustrate box plots of each of stochastic Pareto points of t_{cure} and ΔT_{max} respectively. In addition, the deterministic Pareto front is illustrated with a solid grey line. Pareto fronts of both stochastic and deterministic optimisation are in the form of an L-shape curve dividing the objective space into two different regions. A horizontal region in which cure time can be reduced significantly without considerable changes in exothermic effects and a vertical region in which low temperature overshoot can be reduced significantly with small changes in cure time. The main difference between he stochastic and deterministic Pareto fronts is that the former includes points in which the mean values are dominated by other optimal points, which they dominate then in terms of variability, whilst in deterministic the domination ranking occurs only in terms of nominal values. Also, the mean values of the stochastic Pareto front present higher cure times than the points of the deterministic Pareto front in the case of conservative cure profiles.

The comparison between an optimal point and a standard two dwell profile, as reported in Table 6, illustrates the improvements of stochastic optimisation both in minimisation of mean values and variability. Specifically, the optimal cure profile results in reduction of 13% and 51% in cure time and temperature overshoot in comparison with the standard cure profile, whilst standard deviations are reduced by 66% and 40% respectively.

Cure time shows an overall lower variability than temperature overshoot with the means of coefficient of variation are equal to 2% and 21% for cure time and temperature overshoot respectively. The stochastic Pareto front includes points with cure time values twice as high as for deterministic points. These points are included in the stochastic Pareto front because they present the highest stability in potential fluctuations of process parameters and boundary conditions. These individuals are generated using conservative cure profiles with low first dwell temperature and long first dwell time, therefore the thermal gradients are negligible and the duration of cure long. Moreover, the tip of vertical region of stochastic Pareto front includes one point in which cure time and temperature present high uncertainty with standard deviations of 7 min and 3.6 °C respectively.

The variability of temperature overshoot of points in the vertical region may result in shifting of the stochastic Pareto front in higher or lower values of temperature overshoot than in the deterministic case. In the horizontal region stochastic optimal points present higher temperature overshoots than deterministic points in the range of 3-4 °C. The results obtained with the stochastic optimisation methodology highlight the significant improvements in terms of minimisation both of mean value and variability of cure time and temperature overshoot in comparison with the results of standard cure profiles.

Table 6 Parameters values for optimal points and a standard cure profiles.

Parameter	Optimal point	Standard two-dwell
T_1[°C]	145	160
T_2[°C]	211	180
$dt_1[min]$	65	75

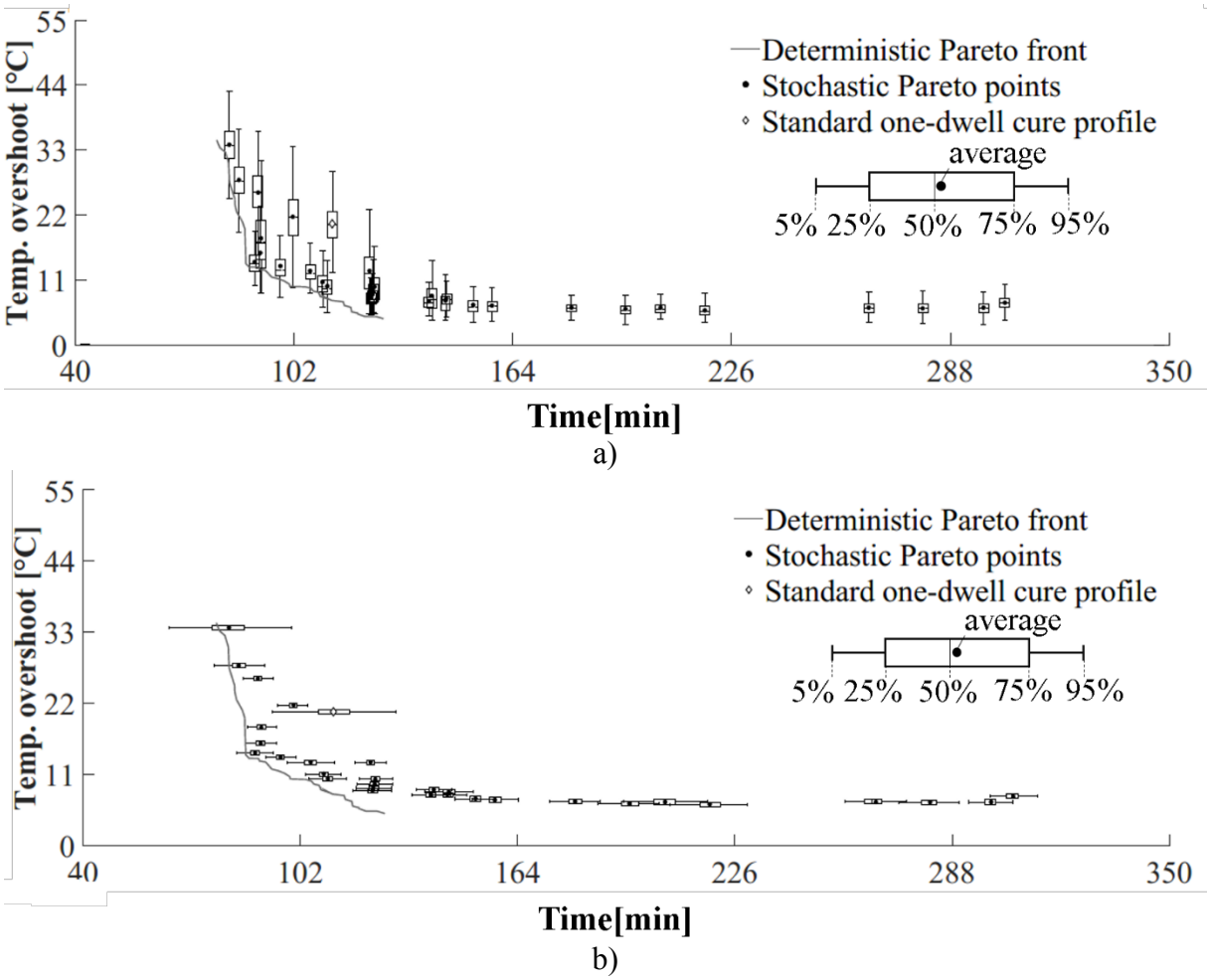

Figure 13 Pareto front of stochastic and deterministic multi-objective optimisation a) cure time box plots; b) temperature overshoot box plots.

4 CONCLUSIONS

The findings of this work highlight the efficient opportunities offered by the stochastic optimisation in terms of eliminating cure time and temperature overshoot uncertainty. The utilisation of stochastic multi-objective optimisation may lead to significant improvements of the composites manufacturing process accomplishing more stable solutions than convention profiles. In addition, the implementation of the stochastic optimisation in the other stages of manufacturing will result in reduction of process duration and thus in minimisation of the cost.

5 ACKNOWLEDGMENTS

This work was supported by the Engineering and Physical Sciences Research Council, through the grant ‘Robustness performance optimisation for automated composites manufacture’ (EP/K031430/1).

REFERENCES

[1] E. Drukker, A. K. Green, and G. Marom, “Mechanical and chemical consequences of through thickness thermal gradients in polyimide matrix composite materials,” *Compos. Part A Appl. Sci. Manuf.*, **34**, 125–133, 2003.

[2] A. A. Skordos and I. K. Partridge, “Inverse heat transfer for optimization and on-line

thermal properties estimation in composites curing.," *Inverse Probl. Sci. Eng.*, **12**, 157–172, 2004.

[3] G. Struzziero and A. A. Skordos, "Multi-objective optimisation of the cure of thick components," *Compos. Part A Appl. Sci. Manuf.*, **93** , 126–136, 2017.

[4] T. S. Mesogitis, A. A. Skordos, and A. C. Long, "Uncertainty in the manufacturing of fibrous thermosetting composites: A review," *Compos. Part A Appl. Sci. Manuf.*, **57**, 67–75, 2014.

[5] T. S. Mesogitis, A. A. Skordos, and A. C. Long, "Stochastic simulation of the influence of cure kinetics uncertainty on composites cure," *Compos. Sci. Technol.*, **110**, 145–151, 2015.

[6] T. S. Mesogitis, A. A. Skordos, and A. C. Long, "Stochastic heat transfer simulation of the cure of advanced composites," *J. Compos. Mater.*, vol. **50**, 2971–2986, 2016.

[7] S. K. Padmanabhan and R. Pitchumani, "Stochastic Analysis of Isothermal Cure of Resin Systems," *Polym. Compos.*, **20**, 73-85, 1999.

[8] C. Acquah, I. Datskov, A. Mawardi, F. Zhang, L. E. K. Achenie, R. Pitchumani, and E. Santos, "Optimization under uncertainty of a composite fabrication process using a deterministic one-stage approach," *Comput. Chem. Eng.*, **30**, 947–960, 2006.

[9] Marc® volume B: Element library. www.mscsoftware.com, 2011.

[10] Marc® volume D: User subroutines and Special Routines. www.mscsoftware.com, 2011.

[11] P. I. Karkanas and I. K. Partridge, "Cure modeling and monitoring of epoxy/amine resin systems. I. Cure kinetics modeling," *J. Appl. Polym. Sci.*, **77**, 1419–1431, 2000.

[12] T. S. Mesogitis, A. A. Skordos, and A. C. Long, "Stochastic simulation of the influence of cure kinetics uncertainty on composites cure," *Compos. Sci. Technol.*, **110**, 145–151, 2015.

[13] J. D. Farmer and E. E. Covert, "Thermal conductivity of a thermosetting advanced composite during its cure," *J. Thermophys. heat Transf.*, **10**, 467–475, 1996.

[14] W. J. C. M. D. McKay R. J. Beckman, "A Comparison of Three Methods for Selecting Values of Input Variables in the Analysis of Output from a Computer Code," *Technometrics*, **21**, 239–245, 1979.

[15] M. A. Oliver and R. Webster, "A tutorial guide to geostatistics : Computing and modelling variograms and kriging," *Catena*, **113**, 56–69, 2014.

[16] S. N. Lophaven, H. B. Nielsen, and J. Søndergaard, "DACE-A Matlab Kriging toolbox, version 2.0," 2002.

[17] RdF®. HFS-A// heat flux sensors. Available at: http:// www.rdfcorp.com.

[18] HexTow®. AS7 carbon fiber. Available at: www.hexcel. com.

[19] A. W. Daniel Fylstra, Leon Lasdon, John Watson, "Design and use of the Microsoft Excel Solver," *Information, Risk Oper. Manag.*, **28**, 29–55, 1998.

[20] W. Smith. "On the simulation and estimation of the mean- reverting Ornstein-Uhlenbeck process," *Commod. Mark. Model.*, 2010.

[21] Hexcel® RTM 6 180°C epoxy system for Resin Transfer Moulding monocomponent system Product Data. www.hexcel.com; 2009.